

Table 1. Detection (DL) and quantification limits (QL) and recoveries (R) of PAHs analyzed by high-performance liquid chromatography (HPLC) with a fluorescence detector.

	Flu	Pyr	BaA	Chry	BjF	BbF	BkF	BaP	DahA	BghiP	IP
DL* (ng m⁻³)	0.018	0.003	0.001	0.001	0.03	0.01	0.001	0.001	0.01	0.015	0.015
QL** (ng m⁻³)	0.06	0.012	0.002	0.002	0.108	0.033	0.004	0.003	0.037	0.050	0.048
R*** (%)	88.3	90.2	101.5	104.1	108.3	96.3	109.2	100.0	89.8	106.7	101.6

* the detection limits were determined as concentration equivalents to three times the signal-to-noise ratio. ** the quantification limits were determined as concentration equivalents to ten times the signal-to-noise ratio. *** the accuracy of the method was determined by analyzing a standard reference material (SRM urban dust 1649b) and expressed as percentage recovery

Table S2. Comparison of PAH mass concentrations in PM₁ particle fraction obtained in this study with other studies.

City, Country	Site description	Sampling period	Average PAH (ng m ⁻³)	Average PM ₁ (µg m ⁻³)	Reference
Zagreb, Croatia	urban background	January–December 2018	Warm season: Flu 0.063; Pyr 0.062; BaA 0.033; Chry 0.074; B _j F 0.076; B _b F 0.131; B _k F 0.052; BaP 0.088; DahA 0.017; B _{ghi} P 0.137; IP 0.120; ΣPAH 0.852 Cold season: Flu 0.631; Pyr 0.627; BaA 0.828; Chry 1.464; B _j F 1.141; B _b F 1.894; B _k F 0.751; BaP 1.454; DahA 0.189; B _{ghi} P 1.556; IP 1.413; ΣPAH 11.815	Warm: 8.7 Cold: 18.6 Annual: 13.6	This study
Zagreb, Croatia	urban background	January 1–February 22, 2014 March 22–May 11, 2014 June 24–August 7, 2014 September 27–November 9, 2014	Winter: Flu 1.214; Pyr 1.210; BaA 0.873; Chry 1.825; B _b F 2.293; B _k F 1.113; BaP 2.228; DahA 0.317; B _{ghi} P 4.199; IP 2.030; ΣPAH 17.274 Spring: Flu 0.219; Pyr 0.151; BaA 0.089; Chry 0.176; B _b F 0.332; B _k F 0.127; BaP 0.205; DahA 0.046; B _{ghi} P 0.650; IP 0.268; ΣPAH 2.262 Summer: Flu 0.023; Pyr 0.024; BaA 0.025; Chry 0.032; B _b F 0.059; B _k F 0.027; BaP 0.030; DahA 0.003; B _{ghi} P 0.116; IP 0.031; ΣPAH 0.372 Autumn: Flu 0.204; Pyr 0.218; BaA 0.197; Chry 0.295; B _b F 0.815; B _k F 0.358; BaP 0.593; DahA 0.105; B _{ghi} P 1.667; IP 0.616; ΣPAH 5.069		[26]
Zagreb, Croatia	urban background	January–December 2013	Flu 0.595; Pyr 0.532; BaA 0.487; Chry 0.925; B _b F 1.034; B _k F 0.408; BaP 0.816; DahA 0.083; B _{ghi} P 1.607; IP 0.819	17.8	[19]
Warsaw, Poland	urban	April 20–June 1, 2015	Flu 2.70; Pyr 0.17; BaA 0.57; Chry 1.21; B _b F 0.36; B _k F 0.26; BaP 1.54; DahA 0.08; B _{ghi} P 0.03; IP 0.09; Σ ₁₆ PAH 8.08		[20]
Gliwice, Poland	urban	April 20–June 1, 2015	Flu 1.56; Pyr 0.57; BaA 1.99; Chry 1.57; B _b F 1.90; B _k F 1.40; BaP 2.72; DahA 0.04; B _{ghi} P 0.52; IP 0.67; Σ ₁₆ PAH 14.85		
Athens Basin, Greece	roadside-industrialized	Selected days in 2008	Flu 0.026; Pyr 0.025; BaA 0.023; Chry 0.069; B _b F 0.254; B _k F 0.143; BaP 0.044; DahA 0.020; B _{ghi} P 0.113; IP 0.168; ΣPAH _{EPA} 0.818	21.8	[21]
Athens Basin, Greece	coastal background	Selected days in 2008	Flu 0.015; Pyr 0.011; BaA 0.020; Chry 0.011; B _b F 0.013; B _k F 0.008; BaP 0.004; DahA 0.004; B _{ghi} P 0.042; IP 0.012; ΣPAH _{EPA} 0.176	16.9	
Katowice, Poland	urban background	August 2, 2009–December 27, 2010	Heating season: Flu 23.36; Pyr 20.30; BaA 17.67; Chry 17.30; B _b F 9.95; B _k F 10.74; BaP 12.48; DahA 0.27; B _{ghi} P 4.95; IP 5.03; Σ ₁₆ PAH 138.74 Non-heating season: Flu 2.01; Pyr 1.87; BaA 7.81; Chry 2.48; B _b F 0.76; B _k F 1.87; BaP 2.97; DahA 0.24; B _{ghi} P 0.05; IP 0.35; ΣPAH ₁₆ 30.26	Heating: 40.70 Non-heating: 20.83	[22]

Złoty Potok, Poland	regional background	August 2, 2009–December 27, 2010	Heating season: Flu 3.42; Pyr 1.86; BaA 2.05; Chry 3.26; BbF 1.55; BkF 1.24; BaP 4.03; IP 0.49; DahA 0.21; BghiP 0.30; Σ_{16} PAH 23.10 Non-heating season: Flu 2.65; Pyr 1.64; BaA 1.57; Chry 2.81; BbF 0.80; BkF 0.68; BaP 2.46; DahA 0.37; BghiP 0.24; IP 0.38; Σ_{16} PAH 18.57	Heating: 16.37 Non-heating: 10.32	
Katowce, Poland	urban traffic	August 2, 2009–December 27, 2010	Heating season: Flu 26.69; Pyr 21.51; BaA 19.02; Chry 19.85; BbF 14.23; BkF 13.80; BaP 14.27; DahA 17.21; BghiP 8.29; IP 5.57; Σ_{16} PAH 186.12 Non-heating season: Flu 3.62; Pyr 10.90; BaA 10.41; Chry 3.86; BbF 3.38; BkF 0.97; BaP 4.73; DahA 4.77; BghiP 0.09; IP 0.51; Σ_{16} PAH 56.02	Heating: 41.55 Non-heating: 18.40	
Gdynia (Baltic Sea), Poland	urbanized coastal zone	January 1–December 31, 2012	BaP only Heating season 3.7 ± 3.9 ; Non-heating season 0.2 ± 0.4 ; Average: 2.6 ± 3.6	Heating: 31.5 Non-heating: 25.2 Annual: 27.5	[23]
Czech Republic:			Σ_{15} PAH		
Mladá Boleslav	urban	Winter 2013	15.6	26.0	
Ostrava-Radvanice	industrial	Winter 2014	60.8	29.4	
Čelákovice	urban	Winter 2015	11.7	17.6	[24]
Kladno-Švermov	urban	Winter 2016	25.5	18.8	
Brno	urban	Winter 2017	20.7	34.2	
Košetice	rural	Winter 2017	12.3	24.5	
Treviso, Veneto region, Italy	Urban background	January–June 2017	Flu 0.52; Pyr 0.73; BaA 0.84; Chry 1.73; Σ BbkF 3.56; BaP 0.86; DahA 0.06; BghiP 1.01; IP 0.52		[25]
Guadalajara Metropolitan Area, Mexico	urban (traffic, industry) and urban residential site	April–June 2015	Flu 0.0114; Pyr 0.0171; BaA 1.47; Chry 1.53; BbF 1.62; BkF 0.541; BaP 0.0947; DahA 0.354; BghiP 0.584; IP 0.498; Σ_{16} PAH 7.25		[27]
Metropolitan Area of Porto Alegre, Brazil	roadside/traffic	August 2011–July 2013	Σ PAH 1.32 (summer) Σ PAH 2.02 (winter)	8.60 11.62	
Metropolitan Area of Porto Alegre, Brazil	urban road/ traffic	August 2011–July 2013	Σ PAH 1.57 (summer) Σ PAH 3.05 (winter)	13.47 17.50	[28]

Table S3. Risk parameters for different age groups.

Definition	Units	Infant	Children	Adults
Inhalation cancer slope factor of BaP (SF_{inh})	kg day mg ⁻¹	3.14	3.14	3.14
Exposure frequency (EF)	day year ⁻¹	252	252	252
Daily exposure level (ED)	µg g ⁻¹	4.8×10 ⁻⁴	8.8×10 ⁻⁴	7.1×10 ⁻⁴
Body weight (BW)	kg	6.79	36.24	59.78
Average time (AT)	day	25550	25550	25550
Inhalation rate (IR)	m ³ day ⁻¹	5.96	24.87	32.74

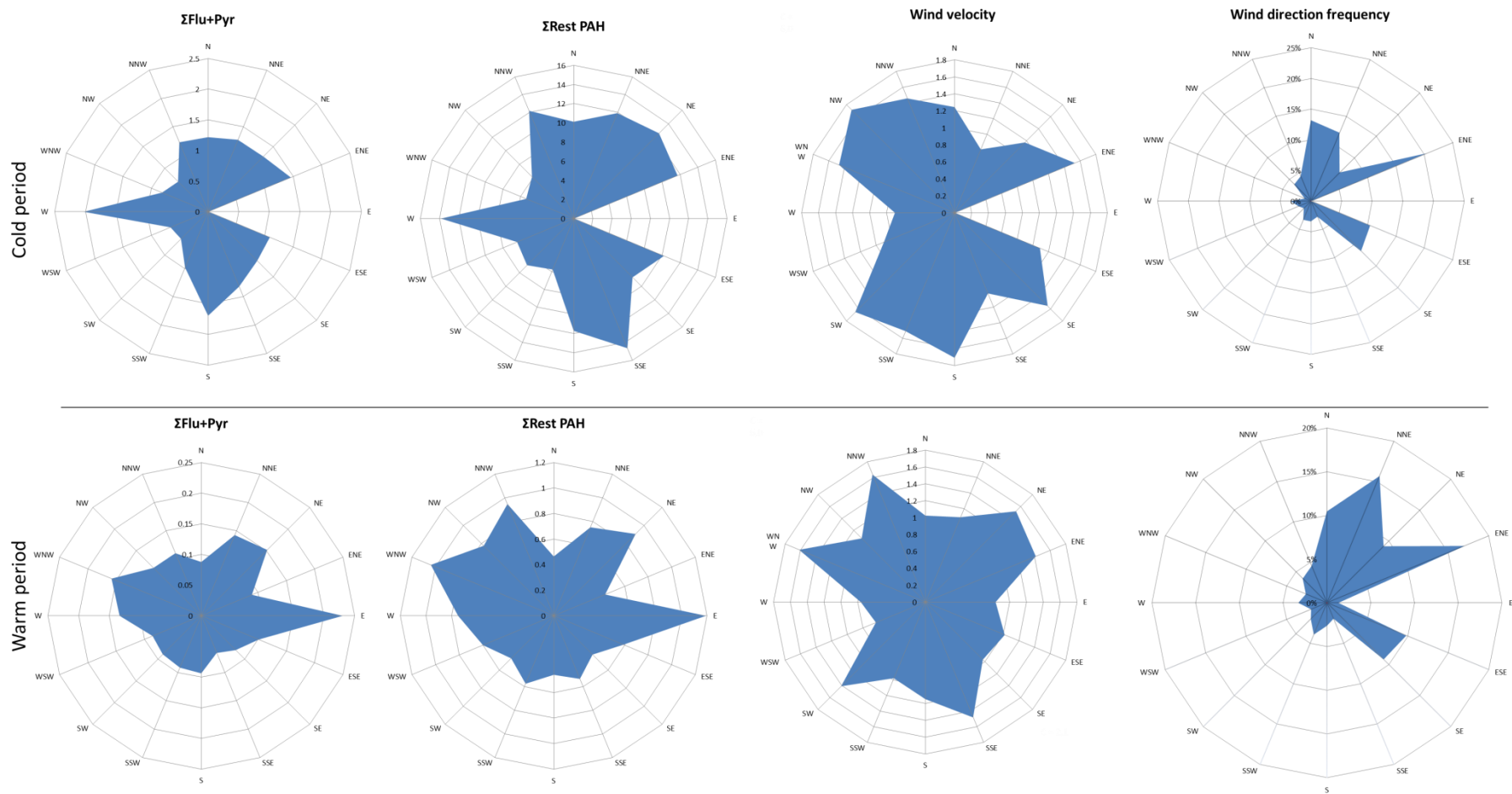
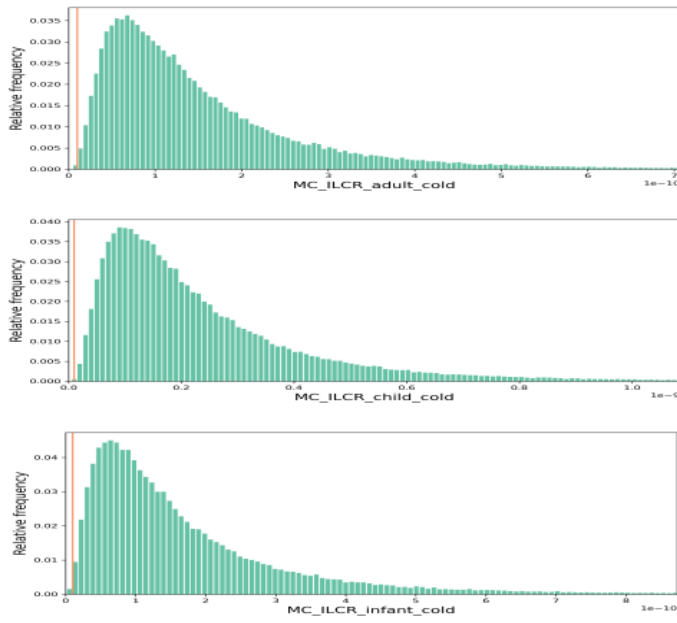


Figure S1. Wind roses. Dependence of PAH concentrations (ng m^{-3}) on wind direction, average wind velocities (m s^{-1}) and wind direction frequencies (%) for cold and warm measuring periods.

Cold period



Warm period

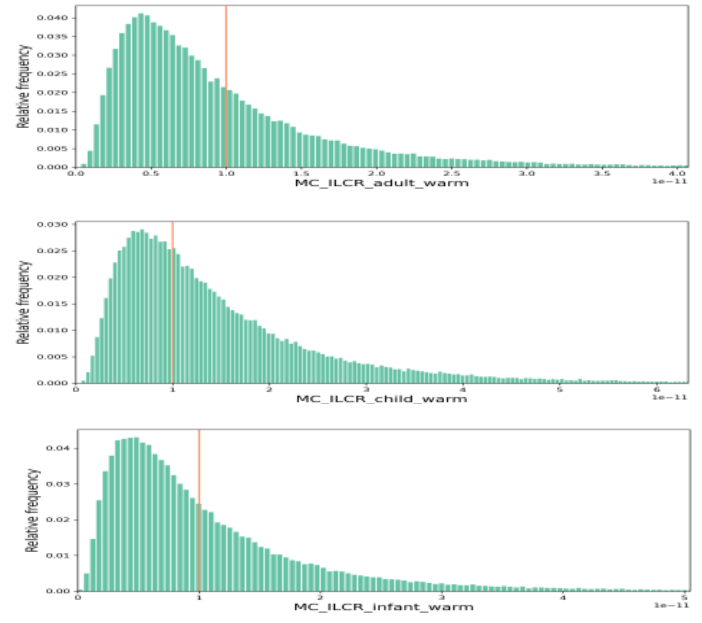


Figure S2. Distribution of incremental lifetime cancer risk for adults, children and infants, derived using Monte Carlo simulation in cold and warm period.